Internal Wave Generation in Lakes with Very Slow Flow

Lee Gordon
NortekUSA
9948 Hibert St. #102
San Diego, California 92131

Atle Lohrmann
Nortek AS
Bruksveien 17
1390 Vollen, Norway

Tobias Jonas
EAWAG
Überlandstrasse 133
CH-8600 Dübendorf, Switzerland

Abstract—A High-Resolution Acoustic Doppler Profiler (HR-ADP), deployed at about 8.5 m depth in Lake Soppensee (Switzerland), observed mean velocities, shear, and internal waves over a depth range of about 4 m. The results suggest that, in spite of maximum velocities less than 15 mm/s, there is shear-induced internal wave generation and mixing around the thermocline. In particular, we observe enhanced internal waves underneath the mixed layer at frequencies bounded by the local buoyancy frequency, and a layer, 0.5-m thick, of critical Richardson's number at the base of the mixed layer.

The HR-ADP is a pulse-to-pulse coherent Doppler sonar which uses a new, more robust means of signal processing to obtain velocity. Based on the noise spectrum, we conclude the measurement uncertainty in this experiment ranges from 0.3 to 1 mm/s.

I. Introduction

Many physical processes in open waters occur at scales or velocities that make them undetectable with conventional Doppler sonars. High-resolution sonars attempt to obtain the ultimate possible performance capability in order to observe these motions. Resulting implementations are both more limiting and more troublesome than conventional Doppler sonars, but the reward is new insight into the physics of underwater flow.

A. High resolution Doppler measurements

Doppler velocity measurement works by observing changing distance to particles in the water, typically by transmitting successive pulses and comparing the echoes [1]. The time required for the echo to return gives an approximate distance to the particles, while phase changes provide a sensitive means to detect small *changes* in this distance. For Doppler measurements to work, phase patterns must be recognizably similar from one ping to the next, that is, the echoes must be correlated.

The precision of velocity observations improves if you increase the echo correlation, and it also improves if you wait longer between pings. Unfortunately, these two means of improvement are at cross-purposes because waiting allows the water to redistribute which then reduces the echo correlation.

Another source of confusion arises as phase changes approach ±180°. A sine wave with phase −180° looks the same as a sine wave with phase +180°. In fact the same problem occurs every time you add or subtract 360° to the phase. The velocity that corresponds to a phase change of 360° is called the ambiguity velocity. If you change the velocity by this ambiguity interval, the phase stays the same. Doppler sonars routinely cope with velocity ambiguity by using various ambiguity resolution methods to determine just how many times the phase has wrapped around 360°. The trouble is that the wrong number of wraps gives you a large velocity error.

Typical Doppler sonars transmit pulse trains such that the echoes from the pulses return combined into a single echo. Mutual interference of the echoes with one another limits correlation to, for example, to 0.5 for pulse pairs. Even single-pulse "incoherent" Doppler sonars can be considered as a limiting case in which two pulses are placed so close together that they become one pulse, twice as long.

Lhermitte [2] explored an approach in which he waited for the first echo to die down before he transmitted the second pulse. This allows the limiting correlation to approach 1.0, and correlation approaching 1.0 dramatically reduces velocity variance (c.f. [3]). Sonars that rely on obtaining correlations near 1.0 are often called "pulse-to-pulse coherent" sonars, and they are often able to achieve velocity variance orders of magnitude lower than in standard incoherent sonars [4]-[7].

B. How the HR-ADP works

Nortek's HR-ADP, introduced in 1998, seeks conditions for high correlation by limiting the product of the maximum velocity and the maximum range. The limit for the 1.5 MHz HR-ADP is around 1 m^2/s—this means a maximum speed of 1 m/s combined with a maximum range of 1 m, or a maximum speed of 25 cm/s combined with a maximum range of 4 m. In practice, the limit varies as much as 25-40% around these values. As velocity increases toward the limit, correlation begins to fall below 1.0. Because small departures of correlation from 1.0 cause large increases in velocity variance, once rising velocity begins to degrade data quality, the data usually quickly becomes unusable.

A second factor in the success of high resolution measurements is out-of-range echoes. Such echoes arise, for example, from inconveniently-placed boundaries or from scattering layers. This requires some care in deployment. One common solution is to place boundaries at the far end of the HR-ADP's profiling range and to take advantage of the signal attenuation incurred by the reflection. The HR-ADP records correlation to enable automatic rejection of bad data.

The HR-ADP requires blanking at the beginning of its range and is subject to sidelobe interference in the last 10% of the range, much the same as in any standard Doppler sonar (c.f. [1]). Careful attention to recovery time in the receiver electronics allows use of relatively short blanking distances (i.e. 7 cm for the 1.5 MHz). Because sidelobe interference near boundaries appears in correlation and echo intensity data as well as the velocity data, you have multiple means to assess sidelobe interference. And it turns out that sidelobe interference is rarely visible in data because the HR-ADP's transducers have narrower beams and sidelobes that are substantially lower than most Doppler sonars.

The HR-ADP transmits two pairs of two pulses each, each pair with a different lag. The different lags extend the maximum measurable velocity a factor of three compared with the use of one pulse pair [4]. Because decorrelation degrades data quality at velocities below the maximum ambiguity velocity, there is no reason to implement ambiguity resolution techniques beyond this limit.

The single most significant improvement implemented in the HR-ADP is the method by which it computes and averages velocity data. Most Doppler sonars compute velocity by first computing the complex autocorrelation (or autocovariance). The complex phase of this autocorrelation provides the phase change with which to compute velocity. Most high-resolution Doppler implementations compute velocity from single pulse pairs, then average computed velocity estimates. Because ambiguity errors are relatively large, they dominate the resulting velocity averages. The HR-ADP, in contrast, averages the complex autocorrelation over multiple ping groups (typically several 10's of ping groups). Because measurements that would incur velocity ambiguity are normally associated with small correlation magnitudes, they are suppressed in the average. It turns out that this method remains robust in oscillatory flow (i.e. waves) in which velocities periodically exceed the ambiguity limits. As long as the true average remains within the HR-ADP's ambiguity limits, the average velocity computed this way remains an unbiased measure of the true velocity.

Because the HR-ADP measures with high precision, it is able to use depth cells as small as 3 cm.

C. 500 kHz vs. 1.5 MHz

The main differences for a 500 kHz HR-ADP include larger transducers, a measurement limit about three times larger (i.e. about 3 m^2/s), 20 cm minimum blanking and 10 cm minimum cell size. Measurement standard deviations for a given bin size also

D. HR-ADP lake deployment

In a recent experiment carried out by EAWAG in Lake Soppensee (Switzerland), a 1.5 MHz HR-ADP observed the fine-scale velocity structure in the mixed layer and thermocline. Flow in this lake is unusually slow—so slow that conventional Doppler sonars could barely resolve differences in the mean flows. The measurements were part of an intensive field experiment designed to investigate convective mixing in natural waters. The lake has no inlet or outlet, and mixing at night is assumed to be purely convective (no wind). The experiment also included measurements of vertical and horizontal temperature microstructure, vertical shear microstructure, CTD-transects, and atmospheric observations from a meteostation deployed on the lake.

The HR-ADP was mounted in a buoyant frame in which the deployment depth was controlled with a winch from shore. The frame was lowered below the mixed layer and the HR-ADP configured to profile upward over a range of 4 meters with 10-cm depth cells. Data were collected every 5 seconds and stored to an internal recorder. Peak velocities were less than 15 mm/s and estimated measurement uncertainty was about 0.2 mm/s. Fig. 1 shows horizontal velocity components; note the relatively strong, uniform flow in the top 1 m and the oscillatory flow in the layers below.

II. Observations.

Fig. 1 shows a relatively uniform layer of flow at the top 1 m of the display, above layers with more variable and oscillatory flow. Fig. 2B supports this with profiles of the mean velocity components. Stratification in a fresh water lake is controlled entirely by the temperature gradient (Fig. 2A); Fig. 2C shows the computed buoyancy frequency N (where $N^2=g/\rho\ (d\rho/dz)$; ρ is density, g is gravity and z is depth) and the velocity gradient, $|\mathbf{du}/dz|$ where **u** is the velocity vector. Fig. 2D shows the computed gradient Richardson's number ($Ri^{1\,2}=N/|(\mathbf{du}/dz)|$). The Richardson's number is a measure of the stability of shear. If $Ri^{1\,2}$ is large, stratification inhibits disturbances—if $Ri^{1\,2}$ is small, turbulence and internal waves grow, dissipate and mix the water. Note that $Ri^{1\,2}$ falls below the critical value 0.5 in

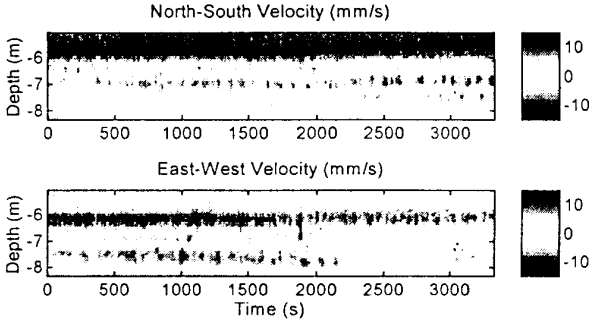

Fig 1. Observed HR-ADP velocity components. The grayscale is designed to emphasize the small-scale oscillatory motions, which are probably internal waves.

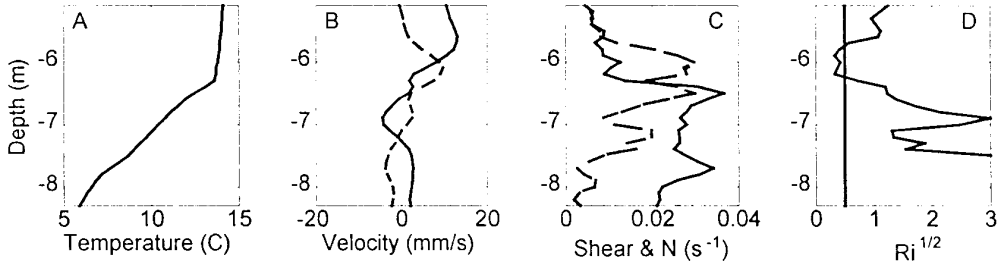

Fig. 2. A Observed temperature and B: velocity profiles (e-w is dashed); C: computed velocity shear (red) and buoyancy frequency (N) and D: computed Richardson's number, Ri1/2 (the dashed line indicates Ri1/2=0.5).

the bottom 0.5 m of the mixed layer—this is where we expect generation of internal waves or turbulence. Fig. 3 shows computed velocity spectra at different depths. The spectra indicate considerable internal wave activity at frequencies below the local buoyancy frequency, N. Internal wave activity is less intense in the mixed layer than in the thermocline.

A. Interpretation

We can divide the flow into four regions.

A) Above –5.8 m. Within the mixed layer, flow is relatively uniform and is also faster than flow below.

B) –5.8 to –6.3 m. At the base of the mixed layer, shear rises and *Ri* falls below the critical value (0.5). Kelvin-Helmholtz instabilities in this layer generate internal waves, which radiate energy and momentum primarily downward.

C) –6.3 to –7.3 m. The most intense internal waves are found at the top of the thermocline. Stratification in this layer supports internal waves better than in the layer above.

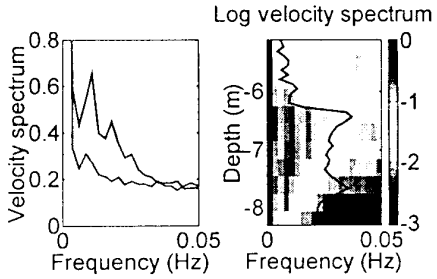

Fig. 3. Velocity spectra. The grayscale contour plot on the right shows spectra vs. depth; the internal wave activity is bounded by the buoyancy frequency, N, plotted with the solid line. The plot on the left compares spectra from within the internal wave region (upper line; depths –6.25 to –7.5 m) with spectra from above this region (lower line; depths –5 to –6 m). Internal waves account for the difference between the two.

D) –7.3 m and below. Internal wave intensity falls even though the stratification stays roughly constant. Assuming the observations represent a quasi-steady state, we could infer that the waves dissipate with distance from the generation region.

We conclude that shear-induced internal waves play a role in the mixing processes of this lake.

III. Measurement Uncertainty.

It is unusual to find sites where velocities are so weak that they fall below the noise floor of an HR-ADP, but this is what we find in Lake Soppensee. Fig. 4 shows velocity spectra from different depths. At frequencies above around 0.04 Hz, the spectra flatten out into noise spectra.

We use the spectrum above 0.06 Hz to estimate the uncertainty, making the assumption that it represents the noise level across the entire spectrum. Then the velocity uncertainty is $(n\,\Delta f)^{1/2}$, where n is the noise level and Δf is 0.1 Hz, or the bandwidth of the entire observed spectrum.

Fig. 5 plots this for both velocity components and beam velocities. Uncertainty increases approximately linearly

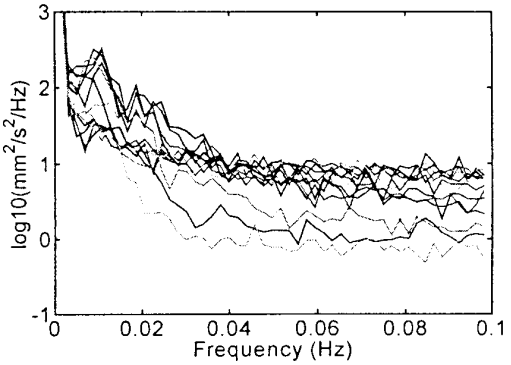

Fig. 4. Velocity spectra at different depths.

with distance from the transducer. There are two possible sources of velocity component uncertainty: instrumental uncertainty (represented by the beam velocity uncertainty), or uncertainty caused by real velocity differences from one beam to the next (or velocity inhomogenieties). We expect inhomogeneous velocities not to play a role because real velocities are smaller than the noise level. The relative levels of the different spectra are consistent with this expectation because:

1) The velocity component uncertainties are approximately proportional to the beam velocity uncertainties.

2) The relative sizes of the uncertainties can be accounted by averaging and trigonometry.

Compared with a conventional incoherent sonar with the same frequency, bin size and ping rate, this observed velocity variance is 10^4 to 10^5 times smaller!

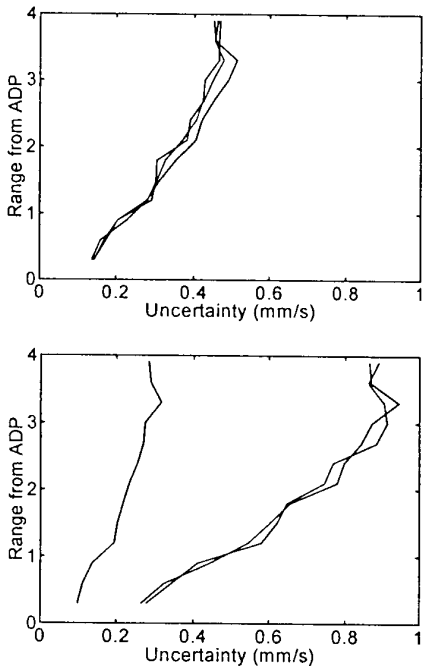

Fig. 5. RMS uncertainty based on spectral levels in the frequency range 0.06-0.1 Hz.

Top. Velocity components. The north-south and east-west velocity component uncertainties are the same while the vertical uncertainty is about 1/3 of the other two.

Bottom. Beam velocity. The beam velocities all have about the same uncertainty. The average beam velocity uncertainty is about 1.5 times larger than the uncertainty of the vertical velocity.

REFERENCES

[1] Gordon, R. L., *Acoustic Doppler Current Profiler Principles of Operation, A Practical Primer, Second Edition for Broadband ADCPs*, RD Instruments, 1996, 51 pp.

[2] R. Lhermitte and R. Serafin, "Pulse-to-pulse coherent Doppler sonar signal processing techniques," *J. Atmos. and Ocean. Technol.*, vol. 1, pp 293-308, 1984.

[3] B. Brumley, R. Cabrera, K. Deines, and E. Terray, "Performance of a broad-band acoustic Doppler current profiler," *IEEE J. Oceanic Eng.*, vol. 16, pp.402-407, 1991.

[4] A. Lohrmann, B. Hackett and L.-P. Roed, High resolution measurements of turbulence, velocity and stress using a pulse-to-pulse coherent sonar, *J. Atmos. and Ocean. Technol.*, vol. 7, pp. 19-37, 1990.

[5] L. Zedel, A. E. Hay, R. Cabrera, and A. Lohrmann, "Performance of a single-beam pulse-to-pulse coherent Doppler profiler," *IEEE J. Oceanic Eng.*, vol. 21, pp.290-297, 1996.

[6] J. T. Sherman and R. Pinkel, Estimates of the vertical wavenumber frequency spectra of vertical shear and strain, *J. Phys. Oceanogr.*, vol. 21, pp 292-303, 1991.

[7] J. T. Sherman, *Observations of the fine scale vertical shear and strain in the upper ocean*, PhD thesis, Scripps Institution of Oceanography, SIO Ref. 89-11, 119 pp., 1989.

Note: you may find this paper, formatted with color illustrations, at the following web address:

www.nortek.no/HR/HR.html